

Information Scrambling and Entanglement Dynamics of Complex Brownian Sachdev-Ye-Kitaev Models

Pengfei Zhang¹

¹*Department of Physics, Fudan University, Shanghai, 200438, China*

January 11, 2023

Abstract

In this work, we study the information scrambling and the entanglement dynamics in the complex Brownian Sachdev-Ye-Kitaev (cBSYK) models, focusing on their dependence on the charge density n . We first derive the effective theory for scramblons in a single cBSYK model, which gives closed-form expressions for the late-time OTOC and operator size. In particular, the result for OTOC is consistent with numerical observations in [1]. We then study the entanglement dynamics in cBSYK chains. We derive the density dependence of the entanglement velocity for both Rényi entropies and the Von Neumann entropy, with a comparison to the butterfly velocity. We further consider adding repeated measurements and derive the effective theory of the measurement induced transition which shows $U(2)_L \otimes U(2)_R$ symmetry for non-interacting models.

Contents

| | | |
|----------|---|-----------|
| 1 | Introduction | 2 |
| 2 | Quantum Information Scrambling at Late Time | 3 |
| 2.1 | Model and two-point functions | 3 |
| 2.2 | Wightman function with sources | 4 |
| 2.3 | Scramblon diagrams and OTOC | 6 |
| 2.4 | Late-time operator size distribution | 8 |
| 3 | Entanglement dynamics and transitions | 10 |
| 3.1 | Model and set-up | 10 |
| 3.2 | Density dependence of entanglement velocity | 12 |
| 3.3 | Measurements and entanglement transitions | 14 |
| 4 | Discussions | 17 |

1 Introduction

Understanding the dynamics of quantum information is of vital importance for revealing the universal picture of quantum many-body systems in both high-energy physics and condensed matter physics. For example, motivated by gravity calculations, the out-of-time-order correlator (OTOC) $\langle W^\dagger(t)V^\dagger(0)W(t)V(0) \rangle$ was introduced to describe the quantum information scrambling in general quantum systems [2–5]. At the early-time regime with $t \ll t_s$, it shows an exponential deviation behavior $1 - \#e^{\lambda t}/N$ in systems with large Hilbert space dimensions, which defines the quantum Lyapunov exponent λ . It has been proved that the quantum Lyapunov has an upper bound $\lambda \leq 2\pi/\beta$ [6], which is saturated by holographic systems dual to semi-classical black holes. The study of information scrambling largely benefits from the Sachdev-Ye-Kitaev (SYK) models [7–10], which describes randomly interacting Majorana fermions. The SYK model can be solved using the $1/N$ expansion. The early-time OTOC in the SYK model is known to show maximally chaotic behavior in the low-temperature limit [7, 9, 10], while its late-time behavior $t \gtrsim t_s$ is described by an emergent bulk scattering with a complex phase shift [11, 12]. Moreover, a series of works study the entanglement of the SYK model, where the Rényi entropies are computed exactly to the leading order of $1/N$ using the perturbation theory or numerical simulations [13–20], which is closely related to replica wormholes in gravity [21–23]. In special limits, results for the Von Neumann can also be obtained by performing the analytical continuation [24–27].

Time scales in quantum information dynamics play an important role in understanding “Planckian” transports in strongly correlated materials [28–34]. Although the original SYK model is defined for Majorana fermions with all-to-all interactions, a number of generalizations have been proposed to study quantum transports, including models with Brownian couplings [35, 36], charge conservations [37–41], or at higher dimensions [42–47]. As an example, authors propose bounds for the Lyapunov exponent in systems with charge conservations motivated by the calculation in complex SYK models [41]. In particular, the Lyapunov exponent and butterfly velocity are computed exactly in the complex Brownian SYK (cBSYK) model. Later, there are attempts to understand the information scrambling in the cBSYK model beyond the early-time regime [1]. By generalizing the mapping from the Majorana Brownian SYK model to the effective bosonic model in [36], authors are able to perform numerical simulations for the OTOC in systems with finite but large N , where a data collapse for OTOC with different charge density n has been observed.

Motivated by these developments, here we push forward the understanding of the quantum information dynamics in the cBSYK model by studying its information scrambling and entanglement dynamics. In section 2, we derive closed-form expressions for the late-time OTOC, which is consistent with numerical observations. We also introduce the idea of finite density operator size and compute its distribution function in the late-time regime. In section 3, we study the entanglement dynamics of cBSYK chains, including the density dependence of the entanglement velocity, and the effective theory for the measurement induced transitions. We conclude our paper in section 4, with discussions for a few future directions.

2 Quantum Information Scrambling at Late Time

In this section, we study the information scrambling of the cBSYK model, focusing on its dependence on charge density n . Adapting the methodology developed in [11, 48, 49], we derive analytical results for the late-time OTOC and operator size distribution by summing up contributions with multiple scramblons. In particular, our results explain the n dependence of OTOC observed in recent numerics [1].

2.1 Model and two-point functions

The complex Brownian SYK model with q -body interactions (cBSYK $_q$) is described by the Hamiltonian:

$$H(t) = \sum_{i_1 < i_2 \dots < i_{\frac{q}{2}} j_1 < j_2 \dots < j_{\frac{q}{2}}} J_{i_1 i_2 \dots i_{\frac{q}{2}} j_1 j_2 \dots j_{\frac{q}{2}}}(t) c_{i_1}^\dagger c_{i_2}^\dagger \dots c_{i_{\frac{q}{2}}}^\dagger c_{j_1} c_{j_2} \dots c_{j_{\frac{q}{2}}}. \quad (1)$$

Here the random interaction parameters $J_{i_1 i_2 \dots i_{\frac{q}{2}} j_1 j_2 \dots j_{\frac{q}{2}}}(t)$ are independent Brownian variables with

$$\overline{J_{i_1 i_2 \dots i_{\frac{q}{2}} j_1 j_2 \dots j_{\frac{q}{2}}}(t)} = 0, \quad \overline{J_{i_1 i_2 \dots i_{\frac{q}{2}} j_1 j_2 \dots j_{\frac{q}{2}}}(t) J_{i_1 i_2 \dots i_{\frac{q}{2}} j_1 j_2 \dots j_{\frac{q}{2}}}(t')^*} = \frac{J \delta(t - t')}{\frac{q}{2}! (\frac{q}{2} - 1)! N^{q-1}}. \quad (2)$$

For the main part of this paper, we assume $q \geq 4$ and the system is many-body chaotic.

The time-dependent Hamiltonian (1) has no energy conservation. Consequently, its steady states are at infinite temperature. Taking $U(1)$ charge conservation into account, the steady-state density matrix reads $\rho = \frac{1}{Z} e^{-\mu Q}$ in the grand canonical ensemble, with total charge $Q = \sum_i c_i^\dagger c_i$. The density of fermions is related to μ by

$$n = \frac{\langle Q \rangle}{N} = \frac{1}{e^\mu + 1} \in [0, 1]. \quad (3)$$

We employ the Keldysh path-integral approach with partition function $\mathcal{Z} = \text{tr} (U(T) \rho U(T)^\dagger)$ and $U(T) = \mathcal{T} e^{-\int_{-T/2}^{T/2} H(t') dt'}$. The path-integral contour includes two branches (u, d), which corresponds to the forward/backward evolution (U, U^\dagger). A pictorial representation for $T \rightarrow \infty$ reads


(4)

The fermion fields ψ_i^s and $\bar{\psi}_i^s$ on the Keldysh contour are labeled by branch indices $s \in \{u, d\}$. We first consider the fermion two-point functions $G^{ss'}(t) = \langle \psi_i^s(t) \bar{\psi}_i^{s'}(0) \rangle$. In the UV limit $t \rightarrow 0^\pm$, $G^{ss'}(t)$ can be determined by the density as

$$G^{ud}(0) = -n, \quad G^{du}(0) = 1 - n, \quad G^{uu}(0^\pm) = G^{dd}(0^\mp) = \frac{1}{2} - n \pm \frac{1}{2}. \quad (5)$$

To the leading order in $1/N$, the self-energy receives contributions from melon diagrams. The Schwinger-Dyson equation then reads

$$\begin{pmatrix} \partial_t - \Sigma^{uu} & -\Sigma^{ud} \\ -\Sigma^{du} & -\partial_t - \Sigma^{dd} \end{pmatrix} \circ \begin{pmatrix} G^{uu} & G^{ud} \\ G^{du} & G^{dd} \end{pmatrix} = I, \quad \Sigma^{ss'} = \text{melon diagram}. \quad (6)$$

Working out the details, we find

$$\begin{aligned}\Sigma^{uu}(t) &= -J\delta(t)G^{uu}(t)^{\frac{q}{2}}(-G^{uu}(-t))^{\frac{q}{2}-1} = -\frac{\Gamma}{2}(1-2n)\delta(t) = \Sigma^{dd}(t), \\ \Sigma^{ud}(t) &= -J\delta(t)G^{ud}(t)^{\frac{q}{2}}(-G^{du}(-t))^{\frac{q}{2}-1} = -\Gamma n\delta(t), \\ \Sigma^{du}(t) &= J\delta(t)G^{du}(t)^{\frac{q}{2}}(-G^{ud}(-t))^{\frac{q}{2}-1} = \Gamma(1-n)\delta(t),\end{aligned}\tag{7}$$

with the decay rate of quasi-particles $\Gamma = J(n(1-n))^{\frac{q}{2}-1}$ [41]. This gives

$$G(t) = \begin{pmatrix} \frac{1}{2} - n + \frac{1}{2}\text{sgn}(t) & -n \\ 1-n & \frac{1}{2} - n - \frac{1}{2}\text{sgn}(t) \end{pmatrix} e^{-\frac{\Gamma|t|}{2}}.\tag{8}$$

Comparing to results in [41], (8) contains no running phase $e^{i\mu t}$, since our evolution Hamiltonian (1) does not include the chemical potential term. It is also useful to work out the retarded and advanced Green's function as

$$G^R(t) = -i\theta(t)\text{tr} \left[\rho \{c_i(t), c_i^\dagger(0)\} \right] = -i\theta(t)(G^{du}(t) - G^{rd}(t)) = -i\theta(t)e^{-\Gamma t/2} = G^A(-t)^*.\tag{9}$$

The dependence of density is only from the decay rate Γ . The result indicates the spectral function $A(\omega) = -2\text{Im}G^R(\omega)$ is Lorentzian, with a single peak near $\omega = 0$.

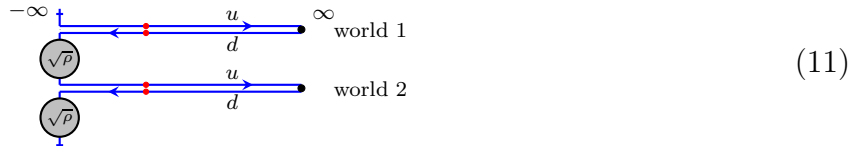
2.2 Wightman function with sources

Now we turn to the study of OTO-correlations. Our final goal is to derive analytical expressions for the out-of-time-order correlators:

$$\begin{aligned}\text{OTOC}_1(t_1, t_2; t_3, t_4) &= -\frac{1}{N^2} \sum_{ij} \text{tr} \left[\sqrt{\rho} c_i(t_1) c_j(t_3) \sqrt{\rho} c_i^\dagger(t_2) c_j^\dagger(t_4) \right], \\ \text{OTOC}_2(t_1, t_2; t_3, t_4) &= -\frac{1}{N^2} \sum_{ij} \text{tr} \left[\sqrt{\rho} c_i^\dagger(t_1) c_j(t_3) \sqrt{\rho} c_i(t_2) c_j^\dagger(t_4) \right].\end{aligned}\tag{10}$$

with $t_1 \approx t_2 \gg t_3 \approx t_4$. Here we choose the convention to equally split the density matrix ρ , while results with other conventions can be computed straightforwardly using our results since ρ commutes with the Hamiltonian. The OTOC can be understood as probing the perturbation distribution excited by operators in the past (t_3, t_4) using operators in the future (t_1, t_2) [50]. A trick proposed in [11] is to replace the actual source with a mean-field perturbation and solve the Wightman function to determine the perturbation generated by a pair of operators, which gives an effective theory of scramblons. OTOCs are then given by combining two Wightman functions.

We first study non-linear equations of Wightman functions on the double Keldysh contour in this subsection. Compared to the traditional Keldysh contour (4), it contains four branches, including two forward evolutions and two backward evolutions. We introduce a "world" label $w \in \{1, 2\}$ in addition to $s \in \{u, d\}$, as indicated in the pictorial representation:



We can introduce Green's functions $G_{ww'}^{ss'}(t) = \langle \psi_i^{sw}(t) \bar{\psi}_i^{s'w'}(0) \rangle$. For $w = w'$, $G_{ww}^{ss'}(t)$ match the single Keldysh result (8) due to the unitarity. For $w \neq w'$, the unitarity implies $G_{ww'}^{ss'}(t)$ is independent of s and s' . Explicitly, we have

$$G_{21}^{ss'}(t) \equiv G_{21}^{W,0}(t) = \sqrt{n(1-n)} e^{-\frac{\Gamma|t|}{2}} \equiv G(t), \quad G_{12}^{ss'}(t) \equiv G_{12}^{W,0}(t) = -G(t). \quad (12)$$

Now we add mean-field sources to probe the perturbation created by fermion operators. We choose a source that does not affect single-world observables, such as $G_{ww}^{ss'}(t)$:

$$\begin{aligned} \delta S = & s_2 \sum_i (\bar{\psi}_i^{u2}(t_0) - \bar{\psi}_i^{d2}(t_0)) (\psi_i^{u1}(t_0) - \psi_i^{d1}(t_0)) \\ & + s_1 \sum_i (\psi_i^{u2}(t_0) - \psi_i^{d2}(t_0)) (\bar{\psi}_i^{u1}(t_0) - \bar{\psi}_i^{d1}(t_0)). \end{aligned} \quad (13)$$

With the source term, the Wightman Green's functions $G_{12/21}^W(t, t')$ show explicit dependence of two time variables, which satisfies the Schwinger-Dyson equation [50]

$$\begin{aligned} \int dt_3 dt_4 G^R(t_{13}) \Sigma_{12}^W(t_3, t_4) G^A(t_{42}) &= G_{12}^W(t_1, t_2), \\ \int dt_3 dt_4 G^R(t_{13}) \Sigma_{21}^W(t_3, t_4) G^A(t_{42}) &= G_{21}^W(t_1, t_2). \end{aligned} \quad (14)$$

Here we have introduced $t_{ij} = t_i - t_j$ for conciseness. The self-energies receive contributions from source terms:

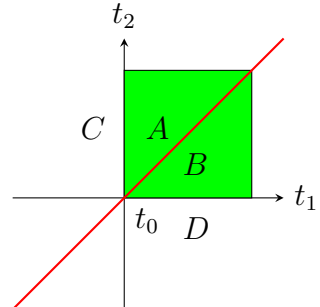
$$\begin{aligned} \Sigma_{21}^W(t, t') &= J\delta(t - t') G_{21}^W(t, t)^{\frac{q}{2}} (-G_{12}^W(t, t))^{\frac{q}{2}-1} - s_2 \delta(t - t_0) \delta(t' - t_0), \\ \Sigma_{12}^W(t, t') &= J\delta(t - t') G_{12}^W(t, t)^{\frac{q}{2}} (-G_{21}^W(t, t))^{\frac{q}{2}-1} + s_1 \delta(t - t_0) \delta(t' - t_0). \end{aligned} \quad (15)$$

Using the explicit form in (9), we can inverse the retarded and advanced Green's functions and obtain differential equations

$$\left(\partial_{t_1} + \frac{\Gamma}{2} \right) \left(\partial_{t_2} + \frac{\Gamma}{2} \right) G_{w\bar{w}}^W(t_1, t_2) = \Sigma_{w\bar{w}}^W(t_1, t_2). \quad (16)$$

Here we have introduced $\bar{w} \neq w$. The right-hand side of these equations only contains delta functions, which separate the solution into different regions as in the Majorana Brownian SYK case [11]. Since the equations (and initial conditions) are symmetric with respect to t_1 and t_2 , we assume

$$\begin{cases} G_{w\bar{w}}^W = e^{-\frac{\Gamma}{2}t_1} f_{w\bar{w}}(t_2) + e^{-\frac{\Gamma}{2}t_2} g_{w\bar{w}}(t_1), & (t_1, t_2) \in A, \\ G_{w\bar{w}}^W = e^{-\frac{\Gamma}{2}t_2} f_{w\bar{w}}(t_1) + e^{-\frac{\Gamma}{2}t_1} g_{w\bar{w}}(t_2), & (t_1, t_2) \in B, \\ G_{w\bar{w}}^W = (-1)^w \sqrt{n(1-n)} e^{-\frac{\Gamma}{2}|t_{12}|}, & (t_1, t_2) \in C \cup D, \\ G_{w\bar{w}}^W(t_0^+, t_0^+) = G_{w\bar{w}}^W(t_0^-, t_0^-) - (-1)^w s_w. \end{cases} \quad (17)$$



For the third line, we use the fact that the source (13) can be neglected due to the cancellation between u and d branches for either $t_1 < t_0$ or $t_2 < t_0$. For the fourth line, we integrate the equation (16) over a small square surrounding (t_0, t_0) and use the continuum condition without the source term $G_{w\bar{w}}^W(t_0^+, t_0^-) = G_{w\bar{w}}^W(t_0^-, t_0^+) = G_{w\bar{w}}^W(t_0^-, t_0^-)$.

To determine the solution of $f_{w\bar{w}}$ and $g_{w\bar{w}}$, we match the boundary condition near the AC and AB boundary. Near the AC boundary we have

$$(\partial_{t_2} + \frac{\Gamma}{2})f_{w\bar{w}}(t_2) = 0, \quad f_{w\bar{w}} = ae^{-\frac{\Gamma t_2}{2}}. \quad (18)$$

We could always fix $a = 0$ using the redundancy of $(f_{w\bar{w}}(t), g_{w\bar{w}}(t)) \rightarrow (f_{w\bar{w}}(t) - ae^{-\frac{\Gamma t}{2}}, g_{w\bar{w}}(t) + ae^{-\frac{\Gamma t}{2}})$. The boundary condition near AB gives

$$\left(\frac{d}{dt} + \Gamma\right)z_{w\bar{w}} = \Gamma z_{w\bar{w}}^{\frac{q}{2}} z_{\bar{w}w}^{\frac{q}{2}-1}, \quad g_{w\bar{w}}(t) = (-1)^w \sqrt{n(1-n)} e^{\frac{\Gamma}{2}t} z_{w\bar{w}}(t). \quad (19)$$

The solution can be parametrized as

$$z_{12} = \frac{C}{(1 + ze^{\varkappa(t-t_0)})^{\frac{1}{q-2}}}, \quad z_{21} = \frac{C^{-1}}{(1 + ze^{\varkappa(t-t_0)})^{\frac{1}{q-2}}}. \quad (20)$$

Here $\varkappa = (q-2)\Gamma$ is the quantum Lyapunov exponent [41]. The initial condition gives

$$1 - \frac{s_2}{\sqrt{n(1-n)}} = \frac{C^{-1}}{(1+z)^{\frac{1}{q-2}}}, \quad 1 - \frac{s_1}{\sqrt{n(1-n)}} = \frac{C}{(1+z)^{\frac{1}{q-2}}}. \quad (21)$$

For small s_1 and s_2 , we expand $\delta C = C - 1$ and z as

$$\delta C = \frac{s_2 - s_1}{\sqrt{n(1-n)}}, \quad z = \frac{q-2}{2} \frac{s_2 + s_1}{\sqrt{n(1-n)}}. \quad (22)$$

We are interested in probing the distribution of scramblons perturbations. As a result, the trick is to take $s_i = p_i e^{\varkappa t_0}$ with $t_0 \rightarrow -\infty$. The final result is

$$G_{w\bar{w}}^W(t_1, t_2) = \frac{G_{w\bar{w}}^{W,0}(t_{12})}{(1 + \tilde{z} e^{\varkappa \frac{t_1+t_2-|t_{12}|}{2}})^{\frac{1}{q-2}}}, \quad \tilde{z} = \frac{q-2}{2} \frac{p_2 + p_1}{\sqrt{n(1-n)}}. \quad (23)$$

Note that the result is symmetric under $p_1 \leftrightarrow p_2$ and $w \leftrightarrow \bar{w}$, which suggests the OTO-correlations are symmetric for particles and holes. This leads to $\text{OTOC}_1 = \text{OTOC}_2 = \text{OTOC}$ in (10). As a result, one may set one of p_i to be zero (we set $p_1 = 0$ and $p_2 = p$), and derive scramblon data using a single source term. This will be explained in the next subsection.

2.3 Scramblon diagrams and OTOC

In the late-time regime, information scrambling is mediated by collective modes named scramblons [10]. In this subsection, we utilize results derived in the last subsection to extract the effective theory of scramblons in the cBSYK model. The OTOC can then be obtained by computing scramblon diagrams.

We begin by examining G^W in the effective theory of scramblons. The result (23) is derived to the leading order of $1/N$ with $-\log p_2 \ll \varkappa t \ll \log N$, which can be identified with diagrams:

$$G_{21}^W(t_1, t_2) = \text{Diagram} = \sum_n \frac{1}{n!} \left(\frac{-2pN e^{\varkappa \frac{t_1+t_2}{2}} \Upsilon^{A,1}(0)}{C} \right)^n \Upsilon^{R,n}(t_{12}). \quad (24)$$

Here each insertion of the source term (13) create a scramblon, giving rise to a propagator $-e^{\varkappa t}/C$ with $C \propto N$. The factor of 2 comes from two possible OTOCs generated by the source term and the factor of N is due to the summation over indices in (13). $\Upsilon^{R/A,n}(t)$ is the vertex function in the future/past between a pair of fermions and n scramblons. Due to the time-reversal symmetry, we have $\Upsilon^{R,n}(t) = \Upsilon^{A,n}(t)$.

Noticing (24) is invariant under $C \rightarrow \lambda^2 C$ and $\Upsilon^{R/A,n} \rightarrow \lambda^n \Upsilon^{R/A,n}$, which reflects an arbitrary rescaling for the definition of scramblons. For simplicity, we fix the convention that

$$\frac{2N}{C} \Upsilon^{A,1}(0) = \frac{q-2}{2\sqrt{n(1-n)}}, \quad (25)$$

which leads to

$$f(x, t) = \sum_n \frac{(-x)^n}{n!} \Upsilon^{R,n}(t) = \frac{G(t)}{(1 + x e^{-\frac{\varkappa}{2}|t|})^{\frac{1}{q-2}}}. \quad (26)$$

Performing the Taylor expansion, we find

$$\Upsilon^{R,n}(t) = G(t) \frac{\Gamma(\frac{1}{q-2} + n)}{\Gamma(\frac{1}{q-2})} e^{-\frac{n\varkappa}{2}|t|} = \Upsilon^{A,n}(t). \quad (27)$$

Together with the convention (25), this fixes

$$\Upsilon^{R,1}(0) = \Upsilon^{A,1}(0) = \frac{\sqrt{n(1-n)}}{q-2}, \quad C = \frac{4Nn(1-n)}{(q-2)^2}. \quad (28)$$

The late-time OTOC is defined for the time regime with $\varkappa t \sim \log N$. To the leading order in $1/N$ expansion, we have

$$\text{OTOC}(t_1, t_2; t_3, t_4) = \text{Diagram} = \sum_n (-\lambda)^n \Upsilon^{R,n}(t_{12}) \Upsilon^{A,n}(t_{34}). \quad (29)$$

Since $f(x, t)$ is analytic expect a branch cut along the negative real axis, we could introduce its inverse Laplace transform $h(x, t)$ as in [11]:

$$f(x, t) = \int dy h(y, t) e^{-xy}, \quad \Upsilon^{R,n}(t) = \int dy h(y, t) y^n. \quad (30)$$

Using (26), we have

$$h(y, t) = \sqrt{n(1-n)} \frac{y^{\frac{1}{q-2}-1}}{\Gamma(\frac{1}{q-2})} e^{-ye^{\frac{\varkappa}{2}|t|}}. \quad (31)$$

This leads to several equivalent expressions for the OTOC:

$$\begin{aligned} \text{OTOC}(t_1, t_2; t_3, t_4) &= \int dy_A dy_R h(y_A, t_{12}) h(y_R, t_{34}) e^{-\lambda y_A y_R} \\ &= \int dy_A h(y_A, t_{12}) f(\lambda y_A, t_{34}) = \int dy_R f(\lambda y_R, t_{12}) h(y_R, t_{34}). \end{aligned} \quad (32)$$

In this first line, the result can be understood as each pair of operators creates perturbations in the future/past with distribution $h(y_{R/A}, t)$, which interact through an Euclidean action $S_{\text{eff}} = \lambda y_A y_R$. In the second line, we integrate out y_R (or y_A), and the pair of operators in the past (future) serves as a probe of perturbations in the future (past), with a probe function $f(\lambda y_{A/R}, t)$. Finally, performing the remaining integral explicitly, we find

$$\text{OTOC}(t_1, t_2; t_3, t_4) = G(t_{12})G(t_{34}) \left[\frac{e^{\frac{\kappa}{2}(|t_{12}|+|t_{34}|)}}{\lambda} \right]^{\frac{1}{q-2}} U\left(\frac{1}{q-2}, 1, \frac{e^{\frac{\kappa}{2}(|t_{12}|+|t_{34}|)}}{\lambda}\right). \quad (33)$$

Here we have introduced $\lambda = \frac{e^{\kappa \frac{t_1+t_2-t_3-t_4}{2}}}{C}$. The result shows that the charge density dependence of $\frac{\text{OTOC}(t_1, t_2; t_3, t_4)}{G(t_{12})G(t_{34})}$ only comes from λ , consistent with the numerical observations in [1]. This extends previous discussions on information scrambling in the cBSYK model to the late-time regime [41].

2.4 Late-time operator size distribution

Finally, we consider the operator size distribution of the cBSYK model. The operator size is defined unambiguously at infinite temperature in the full Hilbert space. In this subsection, we first explain our proposal for extending the definition to systems with charge conservation in the grand canonical ensemble with $\mu \neq 0$, which is an analog of the finite-temperature size for systems with energy conservations [48, 51, 32]. We then derive a concrete formula for the late-time operator size using scramblon diagrams.

We begin with the $\mu = 0$ case. To be concrete, we consider the Heisenberg evolution $c_i(t) = U(t)^\dagger c_i(0) U(t)$. The definition of the operator size is basis dependent. Here we choose the local orthonormal basis $\{O_j^a\} = \{I, c_j + c_j^\dagger, i(c_j - c_j^\dagger), 2c_j^\dagger c_j - 1\}$, and define their operator size as $\{n^a\} = \{0, 1, 1, 2\}$. The operator basis for the total system is given by a tensor product of local basis $O_1^{a_1} O_2^{a_2} \dots O_N^{a_N}$ with an operator size $S = \sum_j n_j^{a_j}$. This definition matches the convention for Majorana fermions [52]. The operator size distribution $P(S)$ of $c_i(t)$ is then defined by

$$c_i(t) = \sum_{\{a_n\}} c_{a_1 a_2 \dots a_N} O_1^{a_1} O_2^{a_2} \dots O_N^{a_N}, \quad P(S) = 2 \sum_{\{a_n\}} |c_{a_1 a_2 \dots a_N}|^2 \delta_{\sum_j n_j^{a_j}, S}. \quad (34)$$

At late-time regime, we take the continuum limit of the operator size by introducing $s \equiv S/N \in [0, 2]$ and $\mathcal{P}(s) \equiv NP(sN)$. It is straightforward to show $\int ds \mathcal{P}(s) = \sum_S P(S) = 2\langle c_j^\dagger c_j \rangle = 1$.

To compute the operator size distribution, we use the trick by introducing an auxiliary system with N complex fermions ξ_j . We first prepare the initial state as a maximally entangled state between c_j and ξ_j . On the occupation basis, we have

$$|I\rangle = \prod_j \otimes \frac{1}{\sqrt{2}} (|01\rangle_j + |10\rangle_j). \quad (35)$$

The state satisfies $(c_j - \xi_j)|I\rangle = (c_j^\dagger + \xi_j^\dagger)|I\rangle = 0$. This motivates us to measure the perturbation of $|I\rangle$ using operator

$$Q_S = \frac{1}{2} \sum_j \left[(c_j^\dagger - \xi_j^\dagger)(c_j - \xi_j) + (c_j + \xi_j)(c_j^\dagger + \xi_j^\dagger) \right]. \quad (36)$$

It is straightforward to show that

$$Q_S|I\rangle = 0, \quad Q_S c_j|I\rangle = c_j|I\rangle, \quad Q_S c_j^\dagger|I\rangle = c_j^\dagger|I\rangle, \quad Q_S(2c_j^\dagger c_j - 1)|I\rangle = 2(2c_j^\dagger c_j - 1)|I\rangle. \quad (37)$$

This shows that the eigenvalue of Q_S matches the definition of operator size. As a result, the generating function of the operator size distribution can be expressed as

$$\mathcal{S}(\nu) = \int ds \mathcal{P}(s) e^{-\nu s} = 2 \langle I | c_j^\dagger(t) e^{-\frac{\nu Q_S}{N}} c_j(t) | I \rangle. \quad (38)$$

Now we generalize above arguments to finite μ . We first consider applying $\sqrt{\rho_c} \equiv \sqrt{\rho} \otimes I$ to $|I\rangle$, which leads to a bias in the Hilbert space

$$|I_\mu\rangle = \sqrt{\rho_c}|I\rangle = \frac{1}{\sqrt{\mathcal{Z}}} \prod_j \otimes \frac{1}{\sqrt{2}} (|01\rangle_j + e^{-\frac{\mu}{2}} |10\rangle_j). \quad (39)$$

Tracing out the auxiliary system leads to the correction density matrix of $\text{tr}_\xi(|I_\mu\rangle\langle I_\mu|) = \rho$. To probe deviations from $|I_\mu\rangle$, we ask which operator annihilates the state. We take a symmetric convention with

$$(e^{\frac{\mu}{4}} c_j - e^{-\frac{\mu}{4}} \xi_j)|I_\mu\rangle = (\rho_c^{\frac{1}{4}} c_j \rho_c^{-\frac{1}{4}} - \rho_\xi^{\frac{1}{4}} \xi_j \rho_\xi^{-\frac{1}{4}})|I_\mu\rangle = \rho_c^{\frac{1}{4}} \rho_\xi^{\frac{1}{4}} (c_j - \xi_j)|I\rangle = 0 \quad (40)$$

Here we have introduced $\rho_\xi \equiv I \otimes e^{\mu \sum_j \xi_j^\dagger \xi_j} / \mathcal{Z}$ and used $\rho_\xi|I\rangle = \rho_c|I\rangle$. Similarly, we have $(e^{-\frac{\mu}{4}} c_j^\dagger + e^{\frac{\mu}{4}} \xi_j^\dagger)|I_\mu\rangle = 0$. As in the $\mu = 0$ case, we introduce the positive semi-definite operator

$$Q_{S\mu} \equiv \frac{\cosh \frac{\mu}{2}}{2} \sum_j \left[(e^{\frac{\mu}{4}} c_j^\dagger - e^{-\frac{\mu}{4}} \xi_j^\dagger)(e^{\frac{\mu}{4}} c_j - e^{-\frac{\mu}{4}} \xi_j) + (e^{-\frac{\mu}{4}} c_j + e^{\frac{\mu}{4}} \xi_j)(e^{-\frac{\mu}{4}} c_j^\dagger + e^{\frac{\mu}{4}} \xi_j^\dagger) \right], \quad (41)$$

and define the finite density operator size of $c_j(t)$ by the generating function

$$\begin{aligned} \mathcal{S}_\mu(\nu) &= \int ds \mathcal{P}_\mu(s) e^{-\nu s} \equiv \frac{\langle I | c_j^\dagger(t) \rho_c^{\frac{1}{4}} \rho_\xi^{\frac{1}{4}} e^{-\frac{\nu Q_{S\mu}}{N}} \rho_c^{\frac{1}{4}} \rho_\xi^{\frac{1}{4}} c_j(t) | I \rangle}{\langle I | c_j^\dagger(t) \rho_c^{\frac{1}{2}} \rho_\xi^{\frac{1}{2}} c_j(t) | I \rangle} \\ &= 2 \cosh \frac{\mu}{2} \langle I | c_j^\dagger(t) \rho_c^{\frac{1}{4}} \rho_\xi^{\frac{1}{4}} e^{-\frac{\nu Q_{S\mu}}{N}} \rho_c^{\frac{1}{4}} \rho_\xi^{\frac{1}{4}} c_j(t) | I \rangle. \end{aligned} \quad (42)$$

In the late-time regime with $\kappa t \sim \log N$, only contributions from scramblon diagrams are important due to the suppression of $1/N$. As in [48], the result can be derived by arguments similar to that of the OTOC: We imagine the insertion of c_j and c_j^\dagger creates the perturbation in the future, whose strength is described by the distribution function $h^R(y, 0)$. This perturbation is probed by the size operator $Q_{S\mu}$ in the past, which has a probe function

$$Q_{S\mu} \approx N \left(1 - 2 \cosh \left(\frac{\mu}{2} \right) f(\lambda y, 0) \right) = N \left(1 - \frac{1}{(1 + \lambda y)^{\frac{1}{q-2}}} \right), \quad \lambda = e^{\kappa t} / C. \quad (43)$$

Here we take the expectation value over $|I_\mu\rangle$ for terms without OTO-correlations. This leads to the result

$$\mathcal{S}_\mu(\nu) = 2 \cosh \frac{\mu}{2} \int dy h(y, 0) e^{-\nu[1-(1+\lambda y)^{-\frac{1}{q-2}}]} = \int dy \frac{y^{\frac{1}{q-2}-1}}{\Gamma(\frac{1}{q-2})} e^{-y} e^{-\nu[1-(1+\lambda y)^{-\frac{1}{q-2}}]}. \quad (44)$$

Performing the inverse Laplace transform, the distribution $\mathcal{P}(s)$ is given by

$$\mathcal{P}_\mu(s) = |y'(s)| \frac{y(s)^{\frac{1}{q-2}-1}}{\Gamma(\frac{1}{q-2})}, \quad s = 1 - (1 + \lambda y)^{-\frac{1}{q-2}} \in [0, 1]. \quad (45)$$

In the early-time regime with $\lambda \ll 1$, the operator size grows exponentially with exponent \varkappa . In the long-time limit, $c_j(t)$ approaches a maximally scrambled operator, which leads to $\mathcal{P}(s) = \delta(s - 1)$, since the standard deviation of the operator size can be neglected to the leading order of $1/N$. Moreover, as for OTOC, the density dependence only comes from the propagator λ of scramblons¹. This generalizes previous results for the late-time operator size distribution of Majorana SYK models [48].

3 Entanglement dynamics and transitions

In this section, we consider the entanglement dynamics of complex Brownian SYK chains. We first consider the unitary evolutions and study the charge dependence of the entanglement velocity for both the Von Neumann entropy and the m -th Rényi entropy. We then add repeated weak measurements, where measurement induced phase transitions [53–66] exist for both interacting and non-interacting models. We derive the effective theory for the transition, with a comparison to its Majorana counterparts [67–70].

3.1 Model and set-up

We extend the cBSYK model (1) to 1-D chains by introducing multiple copies and adding Brownian hopping terms [71]. The Hamiltonian reads

$$\begin{aligned} H(t) = & \sum_x \sum_{i_1 < i_2 \dots < i_{\frac{q}{2}}} \sum_{j_1 < j_2 \dots < j_{\frac{q}{2}}} J_{i_1 i_2 \dots i_{\frac{q}{2}} j_1 j_2 \dots j_{\frac{q}{2}}}^x(t) c_{i_1, x}^\dagger c_{i_2, x}^\dagger \dots c_{i_{\frac{q}{2}}, x}^\dagger c_{j_1, x} c_{j_2, x} \dots c_{j_{\frac{q}{2}}, x} \\ & + \sum_x \left[\sum_{ij} V_{ij}^x(t) c_{i, x+1}^\dagger c_{j, x} + \text{H.C.} \right]. \end{aligned} \quad (46)$$

Here we take the periodic boundary condition with $x \in \{1, 2, \dots, L\}$. Random parameters on different sites are labeled by x and thus independent. The random hopping strength $V_{ij}^x(t)$ are Brownian variables with

$$\overline{V_{ij}^x(t)} = 0, \quad \overline{V_{ij}^x(t) V_{ij}^x(t')^*} = \frac{V}{2N} \delta(t - t'). \quad (47)$$


¹This statement depends on the overall coefficient in the definition of $Q_{S\mu}$. One may change the definition by an overall factor, which leads to a rescale of s .

$$G_x^{ss'}(t) = \langle \psi_i^s(t) \bar{\psi}_i^{s'}(0) \rangle$$
 are still given by (8), with decay rate $\Gamma = J(n(1-n))^{\frac{q}{2}-1} + V$.

In this section, we are interested in the dynamics of the entanglement entropy for pure states. We focus on the setup with an auxiliary fermion chain $\xi_{i,x}$ [71, 16], which is a direct analog of the gravity calculation [72]. The system is prepared in

$$|\psi_0\rangle = \prod_x \otimes |I_\mu\rangle_x, \quad (48)$$

which contains no entanglement between different sites x . The system is then evolved under the Hamiltonian (46), where the entanglement between different sites builds up. We then choose first L_A sites $x \in [1, 2, \dots, L_A]$ as the subsystem A including both $c_{i,x}$ and $\xi_{i,x}$ fermions. The reduced density matrix ρ_A reads

$$\rho_A = \text{tr}_{\bar{A}} U(t) |\psi_0\rangle \langle \psi_0| U(t)^\dagger =$$


$$(49)$$

Here we draw a pictorial representation, which is understood as a path-integral over the corresponding contour [16, 15]. We have omitted the density matrix ρ for simplicity. Dotted lines represent the interaction between A and \bar{A} in the unitary evolution. We are interested in the entropy of ρ_A . The m -th Rényi entropy and the Von Neumann entropy are defined as

$$S_A^{(m)} = -\frac{1}{m-1} \log \text{tr}_A(\rho_A^n), \quad S_A = \lim_{m \rightarrow 1} S_A^{(m)} = -\text{tr}_A(\rho_A \log \rho_A). \quad (50)$$

As an example, for the second and the forth Rényi entropy, we have

$$\text{tr}_A(\rho_A^2) = \text{tr}_A(\rho_A^4) = \quad (51)$$

Here we have world index $w \in \{1, 2, \dots, m\}$. Using the standard SYK technique, to the leading order of $1/N$ the Rényi entropy is given by the G - Σ action:

$$(m-1)\frac{S_A^{(m)}}{N} = \min_{G\Sigma} \sum_x \left\{ -\text{tr} \log \left(\eta_s \delta_{ww'}^{ss'} \partial_t - \Sigma_{ww',x}^{ss'} \right) - \int dt \Sigma_{ww',x}^{ss'}(t,t) G_{w'w,x}^{s's}(t,t) \right. \\ \left. + \int dt \eta_{s'} \eta_s \left[\frac{J}{q} (-G_{w'w,x}^{s's} G_{ww',x}^{ss'})^{\frac{q}{2}} - \frac{V}{2} T_{w_1 w_2}^{xs} T_{w_3 w_4}^{xs'} G_{w_3 w_1, x}^{s's} G_{w_2 w_4, x+1}^{ss'} \right] - C_0 \right\}. \quad (52)$$

Here we have introduced $\eta_u = 1$, $\eta_d = -1$. $T_{ww'}^{xs} = \delta_{ww'}$ except a twist near the boundary between system A and \bar{A} : $T_{ww'}^{LAd} = T_{w'w}^{Ld} = \delta_{w,w'+1}$. The constant C_0 is chosen such that $S_{\emptyset}^{(m)} = 0$. In general, a full analytical study of (52) is impossible, and numerical simulations for its saddle-point equations are employed. In this section, we instead focus on certain limits where analytical formula can be derived, as explained in the following subsections.

3.2 Density dependence of entanglement velocity

In this subsection, we are interested in the entanglement velocity, in particular its density dependence, of the cBSYK chain. The entanglement velocity $v_E^{(m)}$ is defined as the slope of entropy in the early-time regime $S_A^{(m)} \approx 2v_E^{(m)} s_0^{(m)} t$, where $s_0^{(m)} = -N(m-1)^{-1} \log(n^m + (1-n)^m)$ is the maximal entropy density². We focus on small hopping strength V , where $v_E^{(m)}$ can be obtained by a perturbative calculation. Our discussion primarily follows [25], which focuses on static system-bath couplings with Hermitian operators.

We begin with the Rényi entropy with $n > 1$. For $V = 0$, the contour (51) is reduced to n copies of the traditional Keldysh contour (4). As a result, the Green's functions is diagonal in the world index $G_{ww',x}^{ss'}(t) = G^{ss'}(t) \delta_{ww'}$ with $G^{ss'}(t)$ given by (8). Since there is no coupling between different sites, we have $S_A^{(m)} = 0$ for $V = 0$. Now we adding the effect of V perturbatively. The leading order contribution comes from evaluating the V term in (52) using Green's functions with $V = 0$. Due to the unitarity, the only contribution is from boundary terms with $x = L_A$ and $x = L$:

$$S_A^{(m)}(t) = -\frac{mN}{m-1} V \int_0^t dt' \sum_s G^{ss}(t', t') G^{ss}(t', t') = \frac{2mN}{m-1} V n(1-n)t. \quad (53)$$

More generally, in models where nearest neighbor sites are coupled through p -body Brownian term $\sim (c_{x+1}^\dagger c_x)^{p/2}$, we expect $v_E^{(m)} s_0^{(m)} \sim V[n(1-n)]^{\frac{p}{2}}$.

It is also interesting to compare $v_E^{(m)} s_0^{(m)}$ with butterfly velocity v_B . To determine v_B , we generalize the discussion in subsection 2.2 to the SYK chain case. (19) now becomes

$$\left(\frac{d}{dt} + \Gamma_J + \Gamma_V \right) z_{w\bar{w},x} = \Gamma_J z_{w\bar{w},x}^{\frac{q}{2}} z_{\bar{w}w,x}^{\frac{q}{2}-1} + \frac{\Gamma_V}{2} (z_{w\bar{w},x+1}^{\frac{p}{2}} z_{\bar{w}w,x}^{\frac{p}{2}-1} + z_{w\bar{w},x-1}^{\frac{p}{2}} z_{\bar{w}w,x}^{\frac{p}{2}-1}). \quad (54)$$

Here $\Gamma_J = J(n(1-n))^{\frac{q}{2}-1}$ and $\Gamma_V = V(n(1-n))^{\frac{p}{2}-1}$. Now we consider the linearization of above equation $z_{w\bar{w},x} = 1 - \delta z_{w\bar{w},x}$ with $z_{\bar{w}w,x} = z_{w\bar{w},x}$, which gives

$$\frac{d}{dt} \delta z_{w\bar{w},x} = (q-2)\Gamma_J \delta z_{w\bar{w},x} + \frac{p}{2} \frac{\Gamma_V}{2} (\delta z_{w\bar{w},x+1} + \delta z_{w\bar{w},x-1}) + (p-4) \frac{\Gamma_V}{2} \delta z_{w\bar{w},x}. \quad (55)$$

To the leading order of small V , an initial perturbation near $x = 0$ spreads out as

$$\delta z_{w\bar{w},x}(t) \approx \int \frac{dk}{2\pi} e^{(q-2)\Gamma_J t - p\Gamma_V t k^2/2} e^{ikx} \sim e^{(q-2)\Gamma_J t - \frac{x^2}{2\Gamma_V p t}}. \quad (56)$$

This give $v_B = \sqrt{2(q-2)p\Gamma_J \Gamma_V} \sim \sqrt{JV}(n(1-n))^{\frac{p+q}{4}-1}$. We compare $v_E^{(m)}$ with $v_B s_0^{(m)}$. At small density $n \approx 0$ or high density $n \approx 1$, we find

$$v_B s_0^{(m)} \sim (VJ)^{1/2} \frac{mN}{m-1} (n(1-n))^{\frac{p+q}{4}}. \quad (57)$$

For small V , we thus find $v_B \gg v_E^{(m)}$. The result shows that v_B matches the entanglement velocity v_E only for $p = q$ and $V \sim J$.

²Here the factor of 2 is due to the existence of two boundaries in our setup.

Now we consider the entanglement velocity for the Von Neumann entropy S_A . In the limit of $m \rightarrow 1$, it is found that additional loop diagrams contribute [25], which cancels the divergence of (53). For $m = 2$ and $m = 4$, the diagrams read

$$S_A^{(m)} = -\frac{1}{m-1} \log \text{tr}_A(\rho_A^m), \quad S_A = \lim_{m \rightarrow 1} S_A^{(m)} = -\text{tr}_A(\rho_A \log \rho_A). \quad (58)$$

As an example, for the second and the forth Rényi entropy, we have

$$\delta S_A^{(2)} = \text{diagram} \quad 3\delta S_A^{(4)} = \text{diagram} \quad (59)$$

Here the solid black lines represent the fermion Green's function $G^{s\bar{s}}(t)$. There is also a diagram given by the taking charge conjugation of (59). As the next step, one needs to take the disorder average over Brownian variables, which leads to contractions between V_{ij} . An important observation is that if neglect one of the Green's functions (for example the Green's on the blue contour with $w = 1$), the rest part of the diagram, after summation over m , can be represented by an auxiliary Schwinger-Dyson equation³

$$\begin{aligned} \sum_m (m-1)(-1)^{m-1} \delta S_A^{(m)} &= 4N \int_0^t \int_0^t dt_1 dt_2 G^{du}(t_{12}) S_{\text{aug}}^{ud}(t_{21}) \\ &\approx 4Nt \int_{-\infty}^{\infty} \frac{d\omega}{2\pi} G^{du}(\omega) S_{\text{aug}}^{ud}(\omega), \end{aligned} \quad (60)$$

where diagrammatically we have

$$\begin{aligned} S_{\text{aug}}^{s\bar{s}} &= \text{diagram} + \text{diagram} + \dots \\ \frac{s}{G_{\text{aug}}^{s\bar{s}}} &= \frac{s}{G^{s\bar{s}}} + \text{diagram} + \dots \end{aligned} \quad (61)$$

This leads to

$$\begin{aligned} G_{\text{aug}}(\omega)^{-1} &= \begin{pmatrix} 0 & G^{ud}(\omega) \\ G^{du}(\omega) & 0 \end{pmatrix}^{-1} - \begin{pmatrix} 0 & \Sigma_{\text{aug}}^{ud} \\ \Sigma_{\text{aug}}^{du} & 0 \end{pmatrix}, \\ \Sigma_{\text{aug}}^{s\bar{s}} &= \int \frac{d\omega}{2\pi} \frac{V}{2} G_{\text{aug}}^{s\bar{s}}(\omega), \quad S_{\text{aug}}^{s\bar{s}}(\omega) = \Sigma_{\text{aug}}^{s\bar{s}} + \Sigma_{\text{aug}}^{s\bar{s}} G^{ss}(\omega) S_{\text{aug}}^{s\bar{s}}(\omega). \end{aligned} \quad (62)$$

³Here we add a factor $(-1)^{m-1}$. This is due to the gauge transform of fermion modes $c_d \rightarrow -c_d$ on $(m-1)$ red contours if we hope to set Green's functions the same as $G^{ss'}$ in (8). Please see [67] for the details.

In other words, we use $G^{s\bar{s}}$ in (8) as G_0 , and add the effect of V perturbatively. The solution of $\Sigma_{\text{aug}}^{s\bar{s}}$ takes the form of

$$\Sigma_{\text{aug}}^{ud} = -n\sigma, \quad \Sigma_{\text{aug}}^{du} = (1-n)\sigma, \quad \text{with: } \frac{\Gamma V}{2} \sqrt{\frac{1}{\Gamma^2 + 4(1-n)n\Gamma\sigma}} = \sigma. \quad (63)$$

This gives

$$\begin{aligned} \sum_m (m-1)(-1)^{m-1} \delta S_A^{(m)} &= -8Nt \frac{n(1-n)}{V} \sigma^2 \\ &\approx Nt \left\{ -2n(1-n)V + 4[n(1-n)]^2 \frac{V^2}{\Gamma} - 12[n(1-n)]^3 \frac{V^3}{\Gamma^2} \right\} + O(V^4). \end{aligned} \quad (64)$$

Since diagrammatically $\delta S_A^{(m)} \propto V^m$, we have $(m-1)\delta S_A^{(m)} = -NC(m)[Vn(1-n)/\Gamma]^m \Gamma$. In particular, $C(1) = 2$. Unfortunately, we don't find a way to determine the analytical continuation of $C(m)$ near $m = 1$ unambiguously. Combining (64) with (53), we find

$$S_A(t) = 2NVtn(1-n) \log \left(\frac{\Gamma e^{1-C'(1)/2}}{Vn(1-n)} \right). \quad (65)$$

Comparing (65) and (53), we find an additional factor of $-\log[V(1-n)n/\Gamma]$. We expect this is general for systems with large local Hilbert space dimensions. The enhancement of $\log V/\Gamma$ has also been obtained in [25] for couplings with Hermitian operators. We attribute enhancement of $\log n$ at a small density to the different behavior of the maximal entropy:

$$s_0 \approx -Nn \log n, \quad s_0^{(m>1)} \approx -\frac{Nmn}{m-1}. \quad (66)$$

3.3 Measurements and entanglement transitions

In this subsection, we consider adding repeated weak measurement to the cBSYK chain (46). The evolution of the system then becomes non-unitary, which can exhibit measurement induced entanglement phase transitions. We derive the effective theory for the transition, with a comparison to its Majorana counterpart [68, 69].

We first introduce measurements into the cBSYK chain. We consider weak measurements with respect to operator O , which is described by Kraus operators:

$$K_O^0 = 1 - \gamma_O O^\dagger O + O(\gamma^2), \quad K_O^1 = \sqrt{2\gamma_O} O. \quad (67)$$

Here we assume $\gamma \ll 1$. In this section, we focus on the second Rényi entropy, and perform forced measurement by post-selection of outcome 0. For $\gamma_O = \zeta_O \delta t$, the evolution of $\rho \otimes \rho$ due to the measurement then takes the form of imaginary-time evolutions [69]

$$\rho(t + \delta t) \otimes \rho(t + \delta t) \propto e^{-h_I \delta t} \rho(t) e^{-h_I \delta t} \otimes e^{-h_I \delta t} \rho(t) e^{-h_I \delta t}, \quad (68)$$

with $h_I = \zeta_O O^\dagger O$. Adding contributions from measurements with different O and contributions from the unitary part, the total evolution is governed by the non-Hermitian Hamiltonian [67]:

$$H_{\text{tot}}(t) = H(t) - iH_I, \quad H_I = \sum_O \zeta_O O^\dagger O. \quad (69)$$

For complex fermion model, it is natural to measure with respect to the fermion density operator $n_{i,x} = c_{i,x}^\dagger c_{i,x}$. However, choosing $\{O\} = \{n_{i,x}\}$ with $\zeta_O = \zeta$ leads to $H_I = \zeta Q$, which commutes the $H(t)$. As a result, the steady state is always with zero density n for any $\zeta > 0$. To construct a model with non-trivial entanglement transition, we instead take $\{O\} = \{n_{i \in \text{odd}, x}, 1 - n_{i \in \text{even}, x}\}$ and $\zeta_O = \zeta$, as a result, we have

$$H_I = \zeta \sum_{i,x} (-1)^{x-1} c_{i,x}^\dagger c_{i,x} + \text{cons.} \quad (70)$$

With the repeated weak measurements, we consider the same protocol as described in subsection 3.1. The Rényi entropies can still be computed as in (51). The only difference is the replacement:

$$\text{tr log} \left(\eta_s \delta_{ww'} \partial_t - \Sigma_{ww',x}^{ss'} \right) \rightarrow \text{tr log} \left(\delta_{ww'}^{ss'} [\eta_s \partial_t - \zeta (-1)^x] - \Sigma_{ww',x}^{ss'} \right). \quad (71)$$

As pointed out in [68,69], the transitions for the second Rényi entropy can be understood as a topological defect of the replicated Keldysh contour, which contains two disconnected copies of the traditional Keldysh contour (4). A volume-law/area-law entangled phase corresponds to a non-vanishing/vanishing correlation between the u d branches. Following this idea, we first study the Green's functions for the steady state on the single Keldysh contour with $w = 1$. The Schwinger-Dyson equation reads

$$\begin{pmatrix} \partial_t \mp \zeta - \Sigma_{e/o}^{uu} & -\Sigma_{e/o}^{ud} \\ -\Sigma_{e/o}^{du} & -\partial_t \mp \zeta - \Sigma_{e/o}^{dd} \end{pmatrix} \circ \begin{pmatrix} G_{e/o}^{uu} & G_{e/o}^{ud} \\ G_{e/o}^{du} & G_{e/o}^{dd} \end{pmatrix} = I, \quad (72)$$

$$\Sigma_{e/o}^{ss'} = \text{diagram with two vertices connected by a solid line labeled } e/o \text{ and a dashed line labeled } e/o \text{ with arrows} + \text{diagram with two vertices connected by a dashed line labeled } o/e \text{ with arrows}.$$

Here $G_{e/o}^{ss'}$ is the Green's function for even/odd sites. We would focus on the non-interacting limit with $J = 0$, and comment on the interaction effect finally. For $\zeta < V$, the solution takes the forms of

$$G_{e/o}(\omega) = \begin{pmatrix} -i\omega \mp \frac{\zeta}{2} & \frac{V}{2\phi} \sqrt{1 - \frac{\zeta^2}{V^2}} \\ -\frac{V\phi}{2} \sqrt{1 - \frac{\zeta^2}{V^2}} & i\omega \mp \frac{\zeta}{2} \end{pmatrix}^{-1}, \quad (73)$$

or in the time domain:

$$G_{e/o}(t) = \frac{1}{2} \begin{pmatrix} \text{sgn}(t) \mp \frac{\zeta}{V} & -\phi^{-1} \sqrt{1 - \frac{\zeta^2}{V^2}} \\ \phi \sqrt{1 - \frac{\zeta^2}{V^2}} & -\text{sgn}(t) \mp \frac{\zeta}{V} \end{pmatrix} e^{-\frac{V}{2}|t|}. \quad (74)$$

Interestingly, there is a free parameter ϕ , which is not fixed by (72). This is an analog of the density n for the unitary evolution case, which need to be determined by the initial density matrix $\rho = e^{-\mu Q}/\mathcal{Z}$. The solution of (8) indicates we have $\phi = e^{\mu/2}$. We have checked that this matches the numerical results obtained by using methods elaborated in [16,67]. This solution contains non-trivial correlation between u and d branches, and consequently describes a critical phase with logarithmic entanglement entropy. The correlation vanishes as $\sqrt{1 - \zeta/V}$

near $\zeta = V$, indicating a mean-field transition in an area-law entangled phase. The solution for $\zeta \geq V$ reads

$$G_{e/o}(\omega) = \begin{pmatrix} -i\omega \mp (\zeta - \frac{V}{2}) & 0 \\ 0 & i\omega \mp (\zeta - \frac{V}{2}) \end{pmatrix}^{-1}, \quad (75)$$

which gives

$$G_{e/o}(t) = \frac{1}{2} \begin{pmatrix} \text{sgn}(t) \mp 1 & 0 \\ 0 & -\text{sgn}(t) \mp 1 \end{pmatrix} e^{-\frac{2\zeta-V}{2}|t|}. \quad (76)$$

This solution indicates all particles are in even sites while all odd sites are empty. The solution contains no additional parameters, which indicates the steady state for the area-law entangled phase is independent of the initial density matrix ρ .

We are interested in the effective theory for the transition. We start from the area law phase, and consider the fluctuation of $G_{ww',x}^{ss'}(t, t)$ on the replicated Keldysh contour with two worlds. The saddle-point solution of $G_{ww',x}^{ss'}(t, t)$ is given by two copies of (76) as $G_{ww',x}^{ss',0}(t, t) = \delta_{ww'} G_{x \in \text{even/odd}}^{ss'}(0)$. For fluctuations

$$G_{ww',x}^{ss'}(t, t) = G_{ww',x}^{ss',0}(t, t) + \delta g_{ww',x}^{ss'}(t), \quad (77)$$

expanding the $G - \Sigma$ action to the quadratic order gives

$$S = \phi^2 \sum_{ww'} \int \frac{d\omega}{2\pi} \frac{dk}{2\pi} (\delta g_{ww',e}^{ud}, \delta g_{ww',o}^{ud})^* \cdot \begin{pmatrix} 2\zeta - V - i\omega & -V \cos(k) \\ -V \cos(k) & 2\zeta - V + i\omega \end{pmatrix} \cdot (\delta g_{ww',e}^{ud}, \delta g_{ww',o}^{ud})^T. \quad (78)$$

Here we focus on correlations between u and d branches with $-\delta g_{ww',x}^{du} = \phi^2 (\delta g_{ww',x}^{ud})^*$, which is relevant for the entanglement transition. We introduce the symmetric and anti-symmetric components $\delta g_{ww',s/a}^{s\bar{s}} = \frac{1}{\sqrt{2}} (\delta g_{ww',e}^{s\bar{s}} \pm \delta g_{ww',o}^{s\bar{s}})$, and expand for small ω and k . This leads to

$$S = \phi^2 \sum_{ww'} \int \frac{d\omega}{2\pi} \frac{dk}{2\pi} (\delta g_{ww',s}^{ud}, \delta g_{ww',a}^{ud})^* \cdot \begin{pmatrix} 2\zeta - 2V + V k^2/2 & -i\omega \\ -i\omega & 2\zeta \end{pmatrix} \cdot (\delta g_{ww',s}^{ud}, \delta g_{ww',a}^{ud})^T. \quad (79)$$

Now integrate out the anti-symmetric component, we find

$$S = \phi^2 \sum_{ww'} \int \frac{d\omega}{2\pi} \frac{dk}{2\pi} \left(2\zeta - 2V + \frac{V k^2}{2} + \frac{\omega^2}{2\zeta} \right) |\delta g_{ww',s}^{ud}(\omega, k)|^2. \quad (80)$$

For $\zeta - V > 0$, excitations $\delta g_{ww',s}^{ud}$ have positive energy, while for $\zeta - V < 0$, they tend to condense, which leads to a finite correlation between u and d . To make the condensate value finite, we need to introduce the quartic term. The symmetry of fields $\delta g_{ww',s}^{ud}$ becomes explicit if we treat $\delta g_{ww',s}^{ud}$ as a matrix field φ with indices ww' . (80) now becomes

$$S = \phi^2 \int dx dt \left\{ \frac{1}{2\zeta} \text{tr}(\partial_t \varphi^\dagger \partial_t \varphi) + \frac{V}{2} \text{tr}(\nabla \varphi^\dagger \nabla \varphi) + (2\zeta - 2V) \text{tr}(\varphi^\dagger \varphi) \right\}. \quad (81)$$

This action is invariant under $U(2)_L \otimes U(2)_R$, where the matrix field transforms according to $\varphi \rightarrow u_L \varphi u_R^\dagger$. This can be traced back to the $U(2) \otimes U(2)$ invariance of the replicated non-interacting Hamiltonian, similar to the $O(2) \otimes O(2)$ symmetry in the Majorana case [68]. As a

result, there are two natural quartic terms that are consistent with the symmetry:

$$S_{\text{full}} = \int dxdt \left\{ \frac{\phi^2}{2\zeta} \text{tr}(\partial_t \boldsymbol{\varphi}^\dagger \partial_t \boldsymbol{\varphi}) + \frac{V\phi^2}{2} \text{tr}(\nabla \boldsymbol{\varphi}^\dagger \nabla \boldsymbol{\varphi}) + (2\zeta - 2V)\phi^2 \text{tr}(\boldsymbol{\varphi}^\dagger \boldsymbol{\varphi}) \right. \\ \left. + \lambda_1 \phi^4 \text{tr}(\boldsymbol{\varphi}^\dagger \boldsymbol{\varphi})^2 + \lambda_2 \phi^4 \text{tr}(\boldsymbol{\varphi}^\dagger \boldsymbol{\varphi} \boldsymbol{\varphi}^\dagger \boldsymbol{\varphi}) \right\}. \quad (82)$$

We expect $\lambda_2 > 0$, which determines property of the symmetry breaking phase. To see this, we consider the special case with $\boldsymbol{\varphi} = \varphi_1 \mathbf{I} + \varphi_2 \boldsymbol{\sigma}_x$. We have

$$\text{tr}(\boldsymbol{\varphi}^\dagger \boldsymbol{\varphi})^2 = 4(\varphi_1^2 + \varphi_2^2)^2, \quad \text{tr}(\boldsymbol{\varphi}^\dagger \boldsymbol{\varphi} \boldsymbol{\varphi}^\dagger \boldsymbol{\varphi}) = 2(\varphi_1^4 + 3\varphi_1^2 \varphi_2^2 + \varphi_2^4). \quad (83)$$

As a result, for $\lambda_2 > 0$, the repulsion between ϕ_1 and ϕ_2 is larger than the repulsion within each species, and the energy favors $\phi_1 \neq 0, \phi_2 = 0$ or $\phi_1 = 0, \phi_2 \neq 0$, depending on the boundary condition. In particular, for two copies of the traditional Keldysh contour, u and d branches are paired up with each world, and we have $\phi_1 \neq 0$ and $\phi_2 = 0$. The residue symmetry group is then given by $u_L = u_R$, and there are Goldstone modes living on $U(2)_L \otimes U(2)_R / U(2)_+$. This is different from the Majorana case, where Goldstone modes live on $O(2)_L \otimes O(2)_R / O(2)_+ \sim O(2)$. However, we need to point out that in the large- N limit, only the classical configuration with the lowest energy contributes to the entanglement entropy. Even for the cBSYK chain, such a configuration only contains rotations between ϕ_1 and ϕ_2 , which can be parametrized by $u_R = I$ and $u_L = e^{i\theta\sigma_y}$. Consequently, the entanglement entropy shows the same critical behavior as in Majorana SYK models to the leading order in $1/N$ expansion. We expect the signature of the charge conservation show up to the next order of $1/N$.

Finally, we comment on the interaction effects. Perturbatively, the interaction J contributes a term

$$\delta S = \sum_{ww'} \int dxdt \lambda_q \phi^{\frac{q}{2}} |\varphi_{ww'}|^q. \quad (84)$$

For $q \geq 4$, this term breaks $U(2)_{L/R}$ to $Z_2 \times U(1) \times U(1)$. In this case, the entanglement entropy excites no Goldstone mode, which leads to a volume-law entangled phase.

4 Discussions

In this work, we studied the density dependence of the late-time information scrambling and entanglement dynamics in the cBSYK models. Using the Wightman function on a perturbed background, we derive the effective theory between fermions and scramblons for a single-site cBSYK model, which gives analytical results for the late-time OTOC and operator size distribution to the leading order in $1/N$. We then compute the entanglement velocity of the cBSYK chain using perturbative calculations and derive the effective theory for measurement induced transitions with matrix field $\boldsymbol{\varphi}$.

There are many interesting generalizations of the current work. Firstly, it is interesting to consider the late-time information scrambling of cBSYK chains [73]. This requires a complete solution of (54) with a generalization of (23). Secondly, to the leading order of $1/N$, the entanglement entropy for the cBSYK chain with repeated measurements shows the same scaling as its Majorana counterpart. Recently, there is a proposal [74] for considering charge weighted

version of the entanglement entropy. Similar ideas may be useful in measurement induced transitions with charge conservations. Finally, it is interesting to study the information scrambling and entanglement dynamics in models with non-Abelian symmetries.

Acknowledgment

We thank Xiao Chen, Yingfei Gu, Shao-Kai Jian, and Chunxiao Liu for helpful discussions on related topics.

References

- [1] L. Agarwal and S. Xu, *Emergent symmetry in Brownian SYK models and charge dependent scrambling*, *JHEP* **22** (2020) 045, [[2108.05810](#)].
- [2] P. Hayden and J. Preskill, *Black holes as mirrors: Quantum information in random subsystems*, *JHEP* **09** (2007) 120, [[0708.4025](#)].
- [3] Y. Sekino and L. Susskind, *Fast Scramblers*, *JHEP* **10** (2008) 065, [[0808.2096](#)].
- [4] S. H. Shenker and D. Stanford, *Black holes and the butterfly effect*, *JHEP* **03** (2014) 067, [[1306.0622](#)].
- [5] A. Kitaev, *Hidden correlations in the hawking radiation and thermal noise*, in *Talk given at the Fundamental Physics Prize Symposium*, vol. 10, 2014.
- [6] J. Maldacena, S. H. Shenker and D. Stanford, *A bound on chaos*, *JHEP* **08** (2016) 106, [[1503.01409](#)].
- [7] A. Kitaev, “A simple model of quantum holography (part 1), talk at kitp, april 7, 2015.”
- [8] S. Sachdev and J. Ye, *Gapless spin fluid ground state in a random, quantum Heisenberg magnet*, *Phys. Rev. Lett.* **70** (1993) 3339, [[cond-mat/9212030](#)].
- [9] J. Maldacena and D. Stanford, *Remarks on the Sachdev-Ye-Kitaev model*, *Phys. Rev. D* **94** (2016) 106002, [[1604.07818](#)].
- [10] A. Kitaev and S. J. Suh, *The soft mode in the Sachdev-Ye-Kitaev model and its gravity dual*, *JHEP* **05** (2018) 183, [[1711.08467](#)].
- [11] Y. Gu, A. Kitaev and P. Zhang, *A two-way approach to out-of-time-order correlators*, *JHEP* **03** (2022) 133, [[2111.12007](#)].
- [12] D. Stanford, Z. Yang and S. Yao, *Subleading Weingartens*, *JHEP* **02** (2022) 200, [[2107.10252](#)].
- [13] Y. Gu, A. Lucas and X.-L. Qi, *Spread of entanglement in a Sachdev-Ye-Kitaev chain*, *JHEP* **09** (2017) 120, [[1708.00871](#)].

- [14] C. Liu, X. Chen and L. Balents, *Quantum Entanglement of the Sachdev-Ye-Kitaev Models*, *Phys. Rev. B* **97** (2018) 245126, [[1709.06259](#)].
- [15] P. Zhang, *Entanglement Entropy and its Quench Dynamics for Pure States of the Sachdev-Ye-Kitaev model*, *JHEP* **06** (2020) 143, [[2004.05339](#)].
- [16] Y. Chen, X.-L. Qi and P. Zhang, *Replica wormhole and information retrieval in the SYK model coupled to Majorana chains*, *JHEP* **06** (2020) 121, [[2003.13147](#)].
- [17] P. Zhang, C. Liu and X. Chen, *Subsystem Rényi Entropy of Thermal Ensembles for SYK-like models*, *SciPost Phys.* **8** (2020) 094, [[2003.09766](#)].
- [18] K. Su, P. Zhang and H. Zhai, *Page curve from non-Markovianity*, *JHEP* **21** (2020) 156, [[2101.11238](#)].
- [19] A. Haldar, S. Bera and S. Banerjee, *Rényi entanglement entropy of Fermi and non-Fermi liquids: Sachdev-Ye-Kitaev model and dynamical mean field theories*, *Phys. Rev. Res.* **2** (2020) 033505, [[2004.04751](#)].
- [20] Y. Chen, *Entropy linear response theory with non-Markovian bath*, *JHEP* **04** (2021) 215, [[2012.00223](#)].
- [21] G. Penington, S. H. Shenker, D. Stanford and Z. Yang, *Replica wormholes and the black hole interior*, *JHEP* **03** (2022) 205, [[1911.11977](#)].
- [22] A. Almheiri, T. Hartman, J. Maldacena, E. Shaghoulian and A. Tajdini, *The entropy of Hawking radiation*, *Rev. Mod. Phys.* **93** (2021) 035002, [[2006.06872](#)].
- [23] A. Almheiri, T. Hartman, J. Maldacena, E. Shaghoulian and A. Tajdini, *Replica wormholes and the entropy of hawking radiation*, *Journal of High Energy Physics* **05** (2020) 013.
- [24] Y. Chen and P. Zhang, *Entanglement Entropy of Two Coupled SYK Models and Eternal Traversable Wormhole*, *JHEP* **07** (2019) 033, [[1903.10532](#)].
- [25] P. Dadras and A. Kitaev, *Perturbative calculations of entanglement entropy*, *JHEP* **03** (2021) 198, [[2011.09622](#)].
- [26] S.-K. Jian and B. Swingle, *Phase transition in von neumann entanglement entropy from replica symmetry breaking*, *arXiv preprint arXiv:2108.11973* (2021) .
- [27] P. Dadras, *Disentangling the thermofield-double state*, *JHEP* **01** (2022) 075, [[1905.02305](#)].
- [28] S. A. Hartnoll, A. Lucas and S. Sachdev, *Holographic quantum matter*. MIT press, 2018.
- [29] S. Hod, *Universal Bound on Dynamical Relaxation Times and Black-Hole Quasinormal Ringing*, *Phys. Rev. D* **75** (2007) 064013, [[gr-qc/0611004](#)].
- [30] S. A. Hartnoll, *Theory of universal incoherent metallic transport*, *Nature Phys.* **11** (2015) 54, [[1405.3651](#)].

- [31] A. Legros, S. Benhabib, W. Tabis, F. Laliberté, M. Dion, M. Lizaire et al., *Universal t -linear resistivity and planckian dissipation in overdoped cuprates*, *Nature Physics* **15** (2019) 142–147.
- [32] A. Lucas, *Operator size at finite temperature and Planckian bounds on quantum dynamics*, *Phys. Rev. Lett.* **122** (2019) 216601, [[1809.07769](#)].
- [33] M. Blake, *Universal Charge Diffusion and the Butterfly Effect in Holographic Theories*, *Phys. Rev. Lett.* **117** (2016) 091601, [[1603.08510](#)].
- [34] Y. Gu, X.-L. Qi and D. Stanford, *Local criticality, diffusion and chaos in generalized Sachdev-Ye-Kitaev models*, *JHEP* **05** (2017) 125, [[1609.07832](#)].
- [35] P. Saad, S. H. Shenker and D. Stanford, *A semiclassical ramp in SYK and in gravity*, [1806.06840](#).
- [36] C. Sünderhauf, L. Piroli, X.-L. Qi, N. Schuch and J. I. Cirac, *Quantum chaos in the Brownian SYK model with large finite N : OTOCs and tripartite information*, *JHEP* **11** (2019) 038, [[1908.00775](#)].
- [37] R. A. Davison, W. Fu, A. Georges, Y. Gu, K. Jensen and S. Sachdev, *Thermoelectric transport in disordered metals without quasiparticles: The Sachdev-Ye-Kitaev models and holography*, *Phys. Rev. B* **95** (2017) 155131, [[1612.00849](#)].
- [38] K. Bulycheva, *A note on the SYK model with complex fermions*, *JHEP* **12** (2017) 069, [[1706.07411](#)].
- [39] P. Chaturvedi, Y. Gu, W. Song and B. Yu, *A note on the complex SYK model and warped CFTs*, *JHEP* **12** (2018) 101, [[1808.08062](#)].
- [40] Y. Gu, A. Kitaev, S. Sachdev and G. Tarnopolsky, *Notes on the complex Sachdev-Ye-Kitaev model*, *JHEP* **02** (2020) 157, [[1910.14099](#)].
- [41] X. Chen, Y. Gu and A. Lucas, *Many-body quantum dynamics slows down at low density*, *SciPost Phys.* **9** (2020) 071, [[2007.10352](#)].
- [42] Y. Gu, X.-L. Qi and D. Stanford, *Local criticality, diffusion and chaos in generalized Sachdev-Ye-Kitaev models*, *JHEP* **05** (2017) 125, [[1609.07832](#)].
- [43] Y. Gu, A. Lucas and X.-L. Qi, *Energy diffusion and the butterfly effect in inhomogeneous Sachdev-Ye-Kitaev chains*, *SciPost Phys.* **2** (2017) 018, [[1702.08462](#)].
- [44] X.-Y. Song, C.-M. Jian and L. Balents, *Strongly Correlated Metal Built from Sachdev-Ye-Kitaev Models*, *Phys. Rev. Lett.* **119** (2017) 216601, [[1705.00117](#)].
- [45] Y. Chen, H. Zhai and P. Zhang, *Tunable Quantum Chaos in the Sachdev-Ye-Kitaev Model Coupled to a Thermal Bath*, *JHEP* **07** (2017) 150, [[1705.09818](#)].
- [46] P. Zhang, *Dispersive sachdev-ye-kitaev model: Band structure and quantum chaos*, *Physical Review B* **96** (2017) 205138.

- [47] S.-K. Jian and H. Yao, *Solvable sachdev-ye-kitaev models in higher dimensions: from diffusion to many-body localization*, *Physical review letters* **119** (2017) 206602.
- [48] P. Zhang and Y. Gu, *Operator Size Distribution in Large N Quantum Mechanics of Majorana Fermions*, [2212.04358](#).
- [49] P. Zhang and Z. Yu, *Dynamical Transition of Operator Size Growth in Open Quantum Systems*, [2211.03535](#).
- [50] I. L. Aleiner, L. Faoro and L. B. Ioffe, *Microscopic model of quantum butterfly effect: out-of-time-order correlators and traveling combustion waves*, *Annals of Physics* **375** (2016) 378–406.
- [51] X.-L. Qi and A. Streicher, *Quantum epidemiology: operator growth, thermal effects, and syk*, *Journal of High Energy Physics* **08** (2019) 012.
- [52] D. A. Roberts, D. Stanford and A. Streicher, *Operator growth in the SYK model*, *JHEP* **06** (2018) 122, [[1802.02633](#)].
- [53] Y. Li, X. Chen and M. P. A. Fisher, *Quantum zeno effect and the many-body entanglement transition*, *Phys. Rev. B* **98** (Nov, 2018) 205136.
- [54] X. Cao, A. Tilloy and A. D. Luca, *Entanglement in a fermion chain under continuous monitoring*, *SciPost Phys.* **7** (2019) 24.
- [55] Y. Li, X. Chen and M. P. A. Fisher, *Measurement-driven entanglement transition in hybrid quantum circuits*, *Phys. Rev. B* **100** (Oct, 2019) 134306.
- [56] B. Skinner, J. Ruhman and A. Nahum, *Measurement-induced phase transitions in the dynamics of entanglement*, *Phys. Rev. X* **9** (Jul, 2019) 031009.
- [57] A. Chan, R. M. Nandkishore, M. Pretko and G. Smith, *Unitary-projective entanglement dynamics*, *Phys. Rev. B* **99** (Jun, 2019) 224307.
- [58] Y. Bao, S. Choi and E. Altman, *Theory of the phase transition in random unitary circuits with measurements*, *Physical Review B* **101** (Mar, 2020) .
- [59] S. Choi, Y. Bao, X.-L. Qi and E. Altman, *Quantum error correction in scrambling dynamics and measurement-induced phase transition*, *Physical Review Letters* **125** (Jul, 2020) .
- [60] M. J. Gullans and D. A. Huse, *Dynamical purification phase transitions induced by quantum measurements*, *arXiv e-prints* (May, 2019) arXiv:1905.05195, [[1905.05195](#)].
- [61] M. J. Gullans and D. A. Huse, *Scalable probes of measurement-induced criticality*, *Phys. Rev. Lett.* **125** (Aug, 2020) 070606.
- [62] A. Zabalo, M. J. Gullans, J. H. Wilson, S. Gopalakrishnan, D. A. Huse and J. H. Pixley, *Critical properties of the measurement-induced transition in random quantum circuits*, *Phys. Rev. B* **101** (Feb, 2020) 060301.

- [63] Q. Tang and W. Zhu, *Measurement-induced phase transition: A case study in the nonintegrable model by density-matrix renormalization group calculations*, *Phys. Rev. Research* **2** (Jan, 2020) 013022.
- [64] M. Szyniszewski, A. Romito and H. Schomerus, *Entanglement transition from variable-strength weak measurements*, *Phys. Rev. B* **100** (Aug, 2019) 064204.
- [65] L. Zhang, J. A. Reyes, S. Kourtis, C. Chamon, E. R. Mucciolo and A. E. Ruckenstein, *Nonuniversal entanglement level statistics in projection-driven quantum circuits*, *Physical Review B* **101** (Jun, 2020) .
- [66] A. Biella and M. Schiró, *Many-body quantum zeno effect and measurement-induced subradiance transition*, *Quantum* **5** (2021) 528.
- [67] C. Liu, P. Zhang and X. Chen, *Non-unitary dynamics of Sachdev-Ye-Kitaev chain*, *SciPost Phys.* **10** (2021) 048, [2008.11955].
- [68] P. Zhang, S.-K. Jian, C. Liu and X. Chen, *Emergent Replica Conformal Symmetry in Non-Hermitian SYK₂ Chains*, *Quantum* **5** (2021) 579, [2104.04088].
- [69] S.-K. Jian, C. Liu, X. Chen, B. Swingle and P. Zhang, *Measurement-Induced Phase Transition in the Monitored Sachdev-Ye-Kitaev Model*, *Phys. Rev. Lett.* **127** (2021) 140601, [2104.08270].
- [70] P. Zhang, *Quantum entanglement in the Sachdev-Ye-Kitaev model and its generalizations*, *Front. Phys.* **17** (2022) 43201, [2203.01513].
- [71] S.-K. Jian and B. Swingle, *Note on entropy dynamics in the Brownian SYK model*, *JHEP* **03** (2021) 042, [2011.08158].
- [72] A. Almheiri, R. Mahajan and J. Maldacena, *Islands outside the horizon*, [1910.11077](#).
- [73] L. Agarwal, S. Sahu and S. Xu, *Charge transport, information scrambling and quantum operator-coherence in a many-body system with U(1) symmetry*, [2210.14828](#).
- [74] P. M. Tam, M. Claassen and C. L. Kane, *Topological multipartite entanglement in a fermi liquid*, *arXiv preprint arXiv:2204.06559* (2022) .